Neurobiology of Aging 53 (2017) 67–75

Contents lists available at ScienceDirect

Neurobiology of Aging

journal homepage: www.elsevier.com/locate/neuaging

APOE ε4 status is associated with white matter hyperintensities volume accumulation rate independent of AD diagnosis

Carole H. Sudre [a,b,*], M. Jorge Cardoso [a,b], Chris Frost [c], Josephine Barnes [b], Frederik Barkhof [a,d], Nick Fox [b], Sébastien Ourselin [a,b], for the Alzheimer's Disease Neuroimaging Initiative [1]

[a] Translational Imaging Group, Centre for Medical Image Computing, Department of Medical Physics and Biomedical Engineering, University College London, Malet Place Engineering Building, London, UK
[b] Dementia Research Centre, UCL Institute of Neurology, University College London, London, UK
[c] Department of Medical Statistics, London School of Hygiene and Tropical Medicine, Faculty of Epidemiology and Medical Health, University College London, London, UK
[d] Department of Radiology & Nuclear Medicine, VU University Medical Centre, Amsterdam, the Netherlands

ARTICLE INFO

Article history:
Received 2 September 2016
Received in revised form 6 January 2017
Accepted 11 January 2017
Available online 26 January 2017

Keywords:
White matter hyperintensities
APOE
Alzheimer's disease
Longitudinal

ABSTRACT

To assess the relationship between carriage of *APOE* ε4 allele and evolution of white matter hyperintensities (WMHs) volume, we longitudinally studied 339 subjects from the Alzheimer's Disease Neuroimaging Initiative cohort with diagnoses ranging from normal controls to probable Alzheimer's disease (AD). A purpose-built longitudinal automatic method was used to segment WMH using constraints derived from an atlas-based model selection applied to a time-averaged image. Linear mixed models were used to evaluate the differences in rate of change across diagnosis and genetic groups. After adjustment for covariates (age, sex, and total intracranial volume), homozygous *APOE* ε4ε4 subjects had a significantly higher rate of WMH accumulation (22.5% per year 95% CI [14.4, 31.2] for a standardized population having typical values of covariates) compared with the heterozygous (ε4ε3) subjects (10.0% per year [6.7, 13.4]) and homozygous ε3ε3 (6.6% per year [4.1, 9.3]) subjects. Rates of accumulation increased with diagnostic severity; controls accumulated 5.8% per year 95% CI: [2.2, 9.6] for the standardized population, early mild cognitive impairment 6.6% per year [3.9, 9.4], late mild cognitive impairment 12.5% per year [8.2, 17.0] and AD subjects 14.7% per year [6.0, 24.0]. Following adjustment for *APOE* status, these differences became nonstatistically significant suggesting that *APOE* ε4 genotype is the major driver of accumulation of WMH volume rather than diagnosis of AD.

1. Introduction

The *APOE* gene, and specifically its ε4 allelic variant, has an important dose-dependent association with Alzheimer's disease (AD) risk (Verghese et al., 2011). *APOE* ε4 is associated with increased cerebral amyloid plaque deposition and amount of white matter hyperintensities (WMHs).

WMHs are associated with increasing age in apparently healthy elderly subjects and inversely related to executive function and processing speed (Mortamais et al., 2013). They are thought to be a marker of cerebral small vessel disease, and possible pathophysiological explanations for the imaging change include partial ischemia of the tissue and degradation of the blood-brain barrier (Wardlaw et al., 2015). In line with a possible vascular etiology, WMHs are associated with cardiovascular risk factors such as hypertension (Abraham et al., 2016), diabetes (Brundel et al., 2014), and smoking (Power et al., 2015). However, WMH also occur with greater frequency in AD patients (Holland et al., 2008; Provenzano et al., 2013) compared with normal controls. Interestingly, from the point of view of AD, parenchymal WMH can also be related to cerebral amyloid angiopathy (CAA), where amyloid protein affects blood vessel function, potentially impairing the supply of oxygen and nutrients to the brain (Esiri et al., 2015; Greenberg, 2002;

* Corresponding author at: Translational Imaging Group, 8th Floor, Malet Place Engineering Building, University College London, 2 Malet Place, WC1E 7JE London, UK. Tel.: +44 (0) 203 549 5530; fax: +44 (0) 207 679 0255.
E-mail address: carole.sudre.12@ucl.ac.uk (C.H. Sudre).
[1] Data used in preparation of this article were obtained from the Alzheimer's Disease Neuroimaging Initiative (ADNI) database (adni.loni.usc.edu). As such, the investigators within the ADNI contributed to the design and implementation of ADNI and/or provided data but did not participate in analysis or writing of this report. A complete listing of ADNI investigators can be found at: http://adni.loni.usc.edu/wp-content/uploads/how_to_apply/ADNI_Acknowledgement_List.pdf.

0197-4580/
http://dx.doi.org/10.1016/j.neurobiolaging.2017.01.014

Holland et al., 2008; Zipfel et al., 2009). Studies that have investigated the link between WMH and *APOE* status have led to contradictory results (Benedictus et al., 2013; Brickman et al., 2014; Esiri et al., 2015; Kim et al., 2013). Many of those studies, however, were hampered by a cross-sectional design.

We studied the association between *APOE* ε4 status and WMH in a longitudinal framework, for a population with limited cardiovascular risk factors but heterogeneous in terms of AD diagnoses. We used a novel approach for automatic longitudinal WMH lesion segmentation, with the aim of providing greater precision to the assessment of WMH changes and thereby clarifying the relevance of *APOE* ε4 in the accumulation of WMH.

2. Methods

2.1. Data selection

Data used were obtained from the Alzheimer's Disease Neuroimaging Initiative (ADNI) database (adni.loni.usc.edu). The ADNI project was launched in 2003 as a public-private partnership, whose primary goal has been to test whether serial magnetic resonance imaging, positron emission tomography (PET), other biological markers, and clinical and neuropsychological assessment can be combined to measure the progression of mild cognitive impairment (MCI) and early AD. Information about the study can be found at www.adni-info.org. Data collection was approved by each center's Institutional Review Board, and participants gave written informed consent at time of enrolment.

At their initial visit, following clinical and neuropsychological assessment, each subject was given 1 of 4 diagnoses: normal control (NC), early MCI (EMCI), late MCI (LMCI), or probable AD. To be included in the ADNI study, newly recruited participants had to score 4 or below on the modified Hachinski scale for cerebrovascular disease, thereby limiting the range of WMH at baseline. Furthermore, included MCI subjects had to present with an amnestic form of cognitive decline as opposed to a vascular form associated with executive dysfunction.

We selected subjects from the ADNI database using criteria based on available quality scans. Only subjects for whom at least 4 imaging time points with adequate fluid attenuated inversion recovery images were selected. To avoid introducing any preprocessing bias into the analysis, only subjects with T1 scans preprocessed with N3 histogram sharpening and corrected for B1 bias field and gradient nonlinearity were used. Subjects were further excluded if they had poor quality imaging. Fig. 1 presents the flowchart of data selection. According to the ADNI record of adverse events, none of the selected subjects suffered from stroke during the course of the study.

The genotyping for *APOE* was performed at screening visit using DNA extracted by Cogenic using a 3-mL aliquot of EDTA blood, while the level of corticospinal fluid (CSF) Aβ is obtained using the xMAP Luminex platform and the Innogenetics/Fujirebio AlzBio3 immunoassay kits. Further details on the diagnostic procedure, scanning and imaging protocols as well as genotyping and Aβ measurement can be found at http://www.adni-info.org/scientists/ADNIStudyProcedures.aspx.

2.2. Image analysis

We developed a novel fully automatic multimodal lesion segmentation pipeline to jointly analyze all longitudinal imaging time points together. Instead of considering each time point independently and thereby increasing the variability in the longitudinal assessment, an average image was iteratively created. Alignment was achieved through matching intensities of normal tissue in the images in an iterative procedure involving steps of affine and nonrigid registration using jointly the 2 pulse sequences, the fluid attenuated inversion recovery sequence being affinely aligned to the T1-weighted image (Modat et al., 2010, 2014). Based on the results of an existing method (Sudre et al., 2015) applied to the average image, the WMH segmentation at each time point was generated. In brief, this method builds a Bayesian probabilistic data model based on an evolving Gaussian mixture model, which is able to account for observation outliers and incorporates anatomical priors and contextual information for the average appearance model. The model was then further used to constrain the segmentation at each time point. To do so, the model structure (number of Gaussian components) and its associated parameters and resultant segmentation were used to initialize the optimization of the data modeling in the original space of each time point and provide a priori information. Probabilistic lesion maps were obtained from the Gaussian mixture model based on the evaluation of outlierness when compared to the healthy WM and integrated to determine the final WMH volumes.

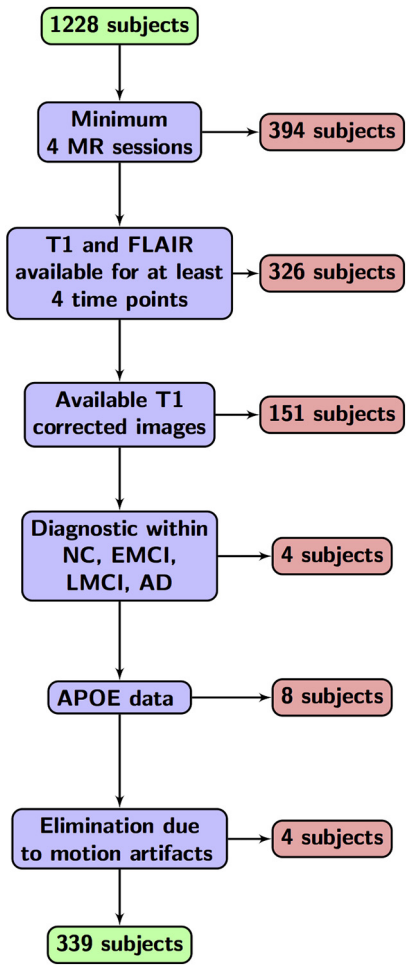

Fig. 1. Flowchart of the subject selection. Red boxes reflect the number of discarded subjects. Abbreviations: AD, Alzheimer's disease; EMCI, early mild cognitive impairment; LMCI, late MCI; NC, normal control. (For interpretation of the references to color in this figure legend, the reader is referred to the Web version of this article.)

Fig. 2 displays the flowchart of the longitudinal framework with its 3 main steps: average image building, probabilistic model selection, and constraint over the individual time points.

The total intracranial volume (TIV), that included total brain volume, ventricles, and CSF between the brain and meninges, was automatically obtained using a previously described method

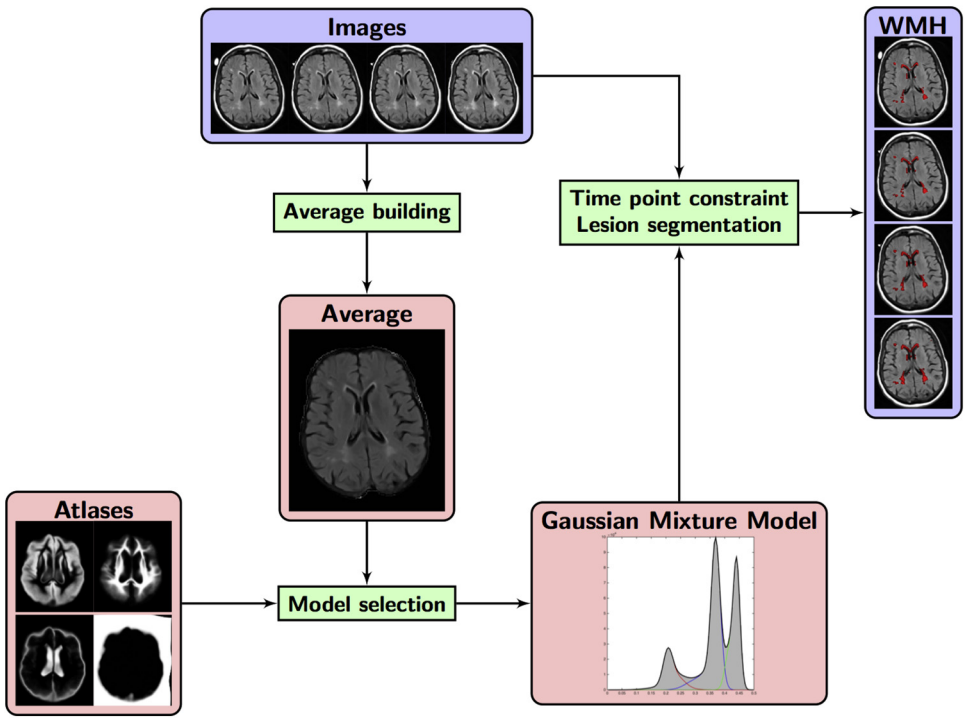

Fig. 2. Flowchart of the longitudinal framework and its 3 main components. The red filled boxes refer to the space of the average image, whereas the blue boxes correspond to the set of individual time point images and the green boxes to performed actions. Abbreviation: WMH, white matter hyperintensity. (For interpretation of the references to color in this figure legend, the reader is referred to the Web version of this article.)

(Cardoso et al., 2015). A single measure of TIV for each individual, generated from the average image, was used as a covariate in statistical analyses.

2.3. Statistical analysis

To assess how our method compared to the first measurements obtained through the method detailed by De Carli et al. (2013) (UC Davis' method) made available on the ADNI database, we calculated Pearson's and Spearman's correlation coefficients. In addition, we assessed agreement between methods through construction of the geometric mean of the ratio of the volumes together with 95% reference ranges. Since differences in volumes may be related to lesion size, we reported these ratios and corresponding reference ranges separately in low versus high lesion volumes (bisected at the median of the mean of the 2 volumes).

All the statistical analyses were performed using Stata 12 v1. Owing to the skewness of the WMH volumes, they were log-transformed before analysis. Cross-sectional analysis of the baseline log-transformed WMH volumes was performed using linear regression models including age, TIV, and sex as covariates in all models. Four models were fitted: these included diagnosis status (model ASTD), genetic status (model ASTG), genetic and diagnosis status (model ASTGD), and genetic status and CSF Aβ 42 concentration (model ASTGAβ) as predictor variables. F-tests were used to assess differences between groups after adjustment for covariates. Fitted group specific means, standardized to a 50/50 mixture of males and females at age 72.2 years with a TIV of 1552 mL (with 95% CI), were also computed and back-transformed. These age and TIV values were chosen as they were the mean values across all subjects.

Longitudinal changes in WMH volume were assessed using linear mixed models, with random intercepts and slopes, for the repeated measures. Linear mixed models, provided that they are properly specified, appropriately allow for the nonindependence of repeated measures from the same subject (Verbeke and Molenberghs, 2000). The dependent variable in all models was the log-transformed volume of WMH with time from initial measurement treated as both a fixed and random effect (thereby allowing slopes to differ between subjects). Other fixed effects were group terms (diagnosis and/or *APOE* status) and group-time interaction terms (thereby allowing mean rates of change to differ between groups) and age, TIV, and sex and their interactions with time. One model (model ASTG) investigated differences in slope between the *APOE* groups, second (model ASTD) differences between the diagnostic groups, and third (model ASTGD) differences according to both of these factors simultaneously. A fourth model (model ASTGAβ) investigated *APOE* status and CSF Aβ 42 concentration as predictors of rates of WMH volume progression. Wald tests were used to compare rates of change between groups after adjustment for covariates. Fitted group-specific mean rates of change (and 95% CI), standardized to a 50/50 mixture of males and females aged 72.2 with a TIV of 1552 mL, were computed and back-transformed from each model.

Both cross-sectional and longitudinal analyses were also performed adding systolic blood pressure and diabetes status as additional covariates, treating these in the same way as age, sex and TIV in all models. However, since hypertension and diabetes are associated with WMH volumes, and are likely on the causal pathway between *APOE* status and WMH levels, these results are presented in supplementary analyses. Finally, in order to understand whether length of follow-up influenced rate of WMH accumulation we added this variable as an additional covariate in all longitudinal models.

3. Results

3.1. Demographic results

The inclusion criteria led to the selection of 339 subjects that collectively had 1620 scans. The number of acquired time points per

Table 1
Demographic findings across *APOE* and diagnostics

Criterion	Diagnosis	*APOE* status					
		32	33	42	43	44	Global
Number total (female)	NC	11 (6)	56 (29)	0 (0)	18 (9)	3 (3)	88 (47)
	EMCI	14 (11)	76 (39)	3 (2)	52 (31)	4 (4)	149 (87)
	LMCI	8 (3)	27 (15)	2 (0)	24 (7)	11 (6)	72 (31)
	AD	0 (0)	9 (6)	1 (1)	14 (9)	6 (5)	30 (21)
	Global	33 (20)	168 (89)	6 (3)	108 (56)	24 (18)	339 (186)
Age, y; mean (SD)	NC	73.3 (6.2)	74.2 (5.8)	/	73 (8)	78.1 (9.7)	74 (6.4)
	EMCI	68.7 (6.6)	71.6 (7.2)	75.3 (5.7)	69.7 (7.2)	68.4 (5.1)	70.7 (7.1)
	LMCI	78.4 (9.5)	71.4 (7.5)	64.3 (2)	71.4 (8.1)	70.6 (7.2)	71.9 (8.1)
	AD	/	78.8 (6)	71.1 (0)	74.6 (7.3)	70.1 (7.2)	74.8 (7.3)
	Global	72.6 (8)	72.8 (7)	71 (6.5)	71.3 (7.7)	71.1 (7.3)	72.2 (7.3)
TIV, mL; mean (SD)	NC	1497 (133)	1530 (169)	/	1543 (152)	1680 (46)	1534 (160)
	EMCI	1604 (167)	1564 (123)	1537 (81)	1565 (165)	1720 (45)	1572 (143)
	LMCI	1579 (148)	1553 (158)	1435 (92)	1516 (201)	1492 (127)	1531 (167)
	AD	/	1568 (178)	1510 (0)	1557 (174)	1537 (131)	1555 (159)
	Global	1562 (155)	1551 (148)	1498 (83)	1549 (171)	1565 (141)	1552 (155)
Study duration, month; mean (SD)	NC	25.8 (3.5)	23.1 (7.4)	/	21.9 (4.9)	25.3 (0.6)	23.3 (6.5)
	EMCI	25.1 (11.7)	26.1 (10.4)	28.3 (16.6)	27.4 (12.1)	30.8 (12.2)	26.6 (11.2)
	LMCI	22.8 (5.8)	23.9 (5.6)	25.5 (0.7)	23.4 (8.1)	19.1 (6)	22.9 (6.6)
	AD	/	14.6 (4.1)	12 (0)	15.8 (5.9)	20.5 (6.2)	16.2 (5.7)
	Global	24.8 (8.2)	24.1 (8.9)	24.7 (12.3)	24.1 (10.4)	22.2 (7.9)	24 (9.3)
Aβ ng/mL; mean [SD; N]	NC	220 (53; 10)	201 (43; 53)	/	173 (42; 15)	111 (42; 3)	194 (48; 81)
	EMCI	216 (42; 10)	198 (47; 73)	115 (0; 1)	170 (48; 50)	121 (14; 3)	187 (50; 137)
	LMCI	193 (43; 8)	196 (45; 26)	129 (51; 2)	138 (33; 23)	114 (31; 11)	162 (51; 70)
	AD	/	156 (52; 9)	/	143 (41; 14)	102 (10; 6)	139 (45; 29)
	Global	211 (46; 28)	196 (46; 161)	125 (37; 3)	160 (45; 102)	111 (26; 23)	179 (52; 317)
WMH, mL; median [IQR]	NC	0.98 [0.72, 1.85]	0.99 [0.54, 2.51]	/	1.38 [0.84, 3.92]	2.07 [1.84, 12.65]	1.10 [0.65, 2.75]
	EMCI	0.77 [0.33, 2.42]	1.23 [0.65, 4.79]	0.40 [0.30, 12.68]	1.69 [0.36, 4.23]	0.90 [0.51, 10.30]	1.23 [0.50, 4.27]
	LMCI	5.55 [3.26, 11.75]	1.70 [0.83, 3.95]	1.62 [0.47–2.76]	0.97 [0.50–4.32]	2.18 [1.04, 6.22]	1.78 [0.73, 5.49]
	AD	/	5.56 [1.88, 6.30]	1.05 [1.05, 1.05]	3.05 [1.33, 5.32]	0.61 [0.30, 3.05]	2.66 [1.06, 5.56]
	Global	1.25 [0.71, 3.95]	1.32 [0.67, 4.21]	0.76 [0.40, 2.76]	1.63 [0.50, 4.26]	1.71 [0.75, 4.15]	1.36 [0.61, 4.25]

Key: AD, Alzheimer's disease; Aβ, Aβ CSF level; EMCI, early mild cognitive impairment; IQR, interquartile range; LMCI, late mild cognitive impairment; N, number; NC, normal controls; SD, standard deviation; TIV, total intracranial volume; WMH, white matter hyperintensity.

subject varied from 4 to 7 (mean 5.15, SD 1.82) and the total length of time from baseline assessment varied from 11 to 52 months (mean 24, SD 9.3). Table 1 shows the demographics of the study population by genetic status and diagnostic group. As expected, the AD subjects had lower CSF Aβ 42 concentrations than control subjects, with the MCI subjects having intermediate values (AD < LMCI < EMCI < NC). CSF Aβ 42 concentrations were lower in subjects with an *APOE* ε4 allele (44 < 42< 43 < 33). Although age was comparable across *APOE* status, EMCI and LMCI were on average younger than NC and AD.

Volumes using our method and the method from UC Davis at first available measurement were strongly associated (Pearson correlation = 0.9, Spearman = 0.95). Absolute volume differences were apparent between methods with our method typically producing smaller values than UC Davis' method. For low lesion volumes, the geometric mean of the ratio was 0.4 with a 95% reference range of [0.1, 1.2]. Analogous results for high volumes (greater than the median) were 0.6 with a 95% reference range of [0.3, 1.1].

3.2. Cross-sectional associations of WMH

The baseline data are summarized in Table 2. There was evidence ($p = 0.016$, model ASTD) that the volume of WMH differed between the diagnosis severity groups, the difference being driven mostly by the low volumes observed in NC compared with the 3 other groups. Although the mean WMH volume in the AD group was slightly lower than that in the EMCI and LMCI groups, these differences were not statistically significant and the 95% confidence interval for the AD group mean was wide, reflecting the fact that this group contains the fewest subjects. Similar results were seen when the differences between the diagnostic groups were adjusted for *APOE* status (p-value from joint test of differences = 0.033, model ASTGD). Considering the Aβ 42 level as a continuous marker also provided evidence of an association ($p<0.0005$) with WMH volume when adjusting for *APOE* (model ASTGAβ).

Across *APOE* status, an increase in WMH volume with the number of ε4 alleles was observed, although this was not statistically significant when *APOE* was considered with or without adjustment for diagnostic group or Aβ. In all these models, the associations with age and TIV were significant ($p < 0.001$), and the gender difference was significant for model ASTG ($p = 0.013$) such that females tended to have more WMH. There was no evidence that diabetes was related to WMH volume, but there was evidence of an association for systolic blood pressure with each 10-mm Hg increase associated with a 12% (95% CI [4.8, 21.1]) increase in volume. The inclusion of these factors as covariates however did not materially alter the pattern of results (see Supplemental Material).

3.3. Models of longitudinal WMH volume change

Table 3 summarizes the results for the longitudinal assessment of the WMH rate of change. Evolution rates are presented as standardized mean values of percentage change in volume per year, with the standardized population being a 50:50 mix of males and females having the mean value of age and TIV across all participants.

There was strong evidence ($p = 0.0002$) that mean rates of change differed between the *APOE* groups with the largest mean rate in the *APOE* ε4ε4 group and the lowest in the *APOE* ε4ε2 group. The standardized mean rate in the *APOE* ε4ε4 group (22.5%/year CI [14.4–31.2]) was significantly higher than that in each of the other groups (10.0%/year [6.7–13.4] in the ε4ε3 group and 6.6%/year [4.1, 9.3] in the ε3ε3 group, 2.8%/year [−2.6 to 8.5] in the ε3ε2 group and −3.2%/year [−14.8 to 9.9] in the ε4ε2 group). The rates in the

Table 2
Baseline models: effects of covariates on differences in WMH volumes across diagnostic groups and *APOE* genotypes when adjusting for age, sex, and TIV

Models	Number (Aβ)	APOE					Diagnosis			
		32	33	42	43	44	NC	EMCI	LMCI	AD
		33 (28)	168 (161)	6 (3)	108 (102)	24 (23)	88 (81)	149 (137)	72 (70)	30 (29)
ASTG	Mean, CI	1.54 [1.06, 2.23]	1.44 [1.22, 1.70]	1.42 [0.59, 3.40]	1.69 [1.37, 2.07]	2.12 [1.36, 3.29]			NA	
	Overall *p*-value	0.5069								
	Pairwise	/								
ASTD	Mean, CI			NA			1.15 [0.92, 1.44]	1.67 [1.40, 2.00]	1.92 [1.49, 2.46]	1.71 [1.15, 2.52]
	Overall *p*-value						0.0157			
	Pairwise						EMCI versus NC*; LMCI versus NC**			
ASTGD	Mean, CI	1.57 [1.07, 2.30]	1.49 [1.23, 1.80]	1.28 [0.54, 3.04]	1.64 [1.32, 2.03]	1.98 [1.27, 3.08]	1.17 [0.86, 1.59]	1.70 [1.31, 2.21]	1.88 [1.39, 2.52]	1.64 [1.07, 2.52]
	Overall *p*-value	0.7786					0.0331			
	Pairwise	/					EMCI versus NC*; LMCI versus NC**			
ASTGAβ	Mean, CI	2.09 [1.38, 3.15]	1.58 [1.33, 1.89]	1.08 [0.31, 3.73]	1.50 [1.21, 1.87]	1.49 [0.91, 2.41]			NA	
	Overall *p*-value	0.6996								
	Pairwise	/								

p-values: $^{*}p < 0.05$; $^{**}p < 0.01$.
Values are for a standardized 50/50 mixture of males and females at age 72.2 y with a TIV of 1552 mL. Results are presented back-transformed to their original scale.
Model covariates: ASTD, age sex TIV diagnosis; ASTG, age sex TIV genetic status; ASTGAβ, age sex TIV genetic status Aβ level; ASTGD, age sex TIV diagnosis genetic status. Key: AD, Alzheimer's disease; CI, confidence interval; EMCI, early mild cognitive impairment; LMCI, late mild cognitive impairment; NA, not applicable; NC, normal control; TIV, total intracranial volume.

Table 3
Longitudinal models: effect of baseline predictors on differences in WMH volume change when adjusting for age, sex, and TIV

Models	Number (Aβ)	APOE					Diagnosis			
		32	33	42	43	44	NC	EMCI	LMCI	AD
		33 (28)	168 (161)	6 (3)	108 (102)	24 (23)	88 (81)	149 (137)	72 (70)	30 (29)
ASTG	%Change/year CI	2.80 [−2.58, 8.47]	6.64 [4.09, 9.26]	−3.21 [−14.76, 9.91]	9.98 [6.66, 13.40]	22.54 [14.43, 31.22]			NA	
	Overall *p*-value	0.0002								
	Pairwise	32 versus 43*; 32 versus 44***; 33 versus 44***; 42 versus 44**; and 43 versus 44**								
ASTD	%Change/year CI			NA			5.81 [2.15, 9.59]	6.57 [3.86, 9.36]	12.54 [8.24, 17.02]	14.65 [5.97, 24.03]
	Overall *p*-value						0.0303			
	Pairwise						EMCI versus LMCI*; NC versus LMCI*			
ASTGD	%Change/year CI	3.88 [−1.91, 10.01]	7.96 [4.65, 11.36]	−3.21 [−14.82, 9.98]	10.76 [7.00, 14.65]	21.69 [13.63, 30.31]	5.25 [0.56, 10.16]	5.92 [1.99, 10.00]	10.80 [5.96, 15.87]	9.76 [1.09, 19.17]
	Overall *p*-value	0.0016					0.1811			
	Pairwise	32 versus 43*; 32 versus 44***; 33 versus 44**; 42 versus 43*; 42 versus 44**; 43 versus 44*					/			
ASTGAβ	%Change/year CI	6.10 [0.24, 12.32]	7.21 [4.54, 9.95]	−10.59 [−24.53 , 5.92]	9.16 [5.79, 12.63]	20.22 [11.79, 29.28]			NA	
	Overall *p*-value	0.0061								
	Pairwise	32 versus 44*; 33 versus 44**; 42 versus 43*; 42 versus 44**; 43 versus 44*								

p-values: $^{*}p < 0.05$; $^{**}p < 0.01$; $^{***}p < 0.001$.
Standardized percentage changes are presented along with the confidence intervals. Values are standardized to a 50/50 mixture of males and females of age 72.2 y with a TIV of 1552 mL.
Model covariates: ASTD, age sex TIV diagnosis; ASTG, age sex TIV genetic status; ASTGAβ, age sex TIV genetic status Aβ level; ASTGD, age sex TIV diagnosis genetic status. Key: AD, Alzheimer's disease; CI, confidence interval; EMCI, early mild cognitive impairment; LMCI, late mild cognitive impairment; NA, not applicable; NC, normal control; TIV, total intracranial volume.

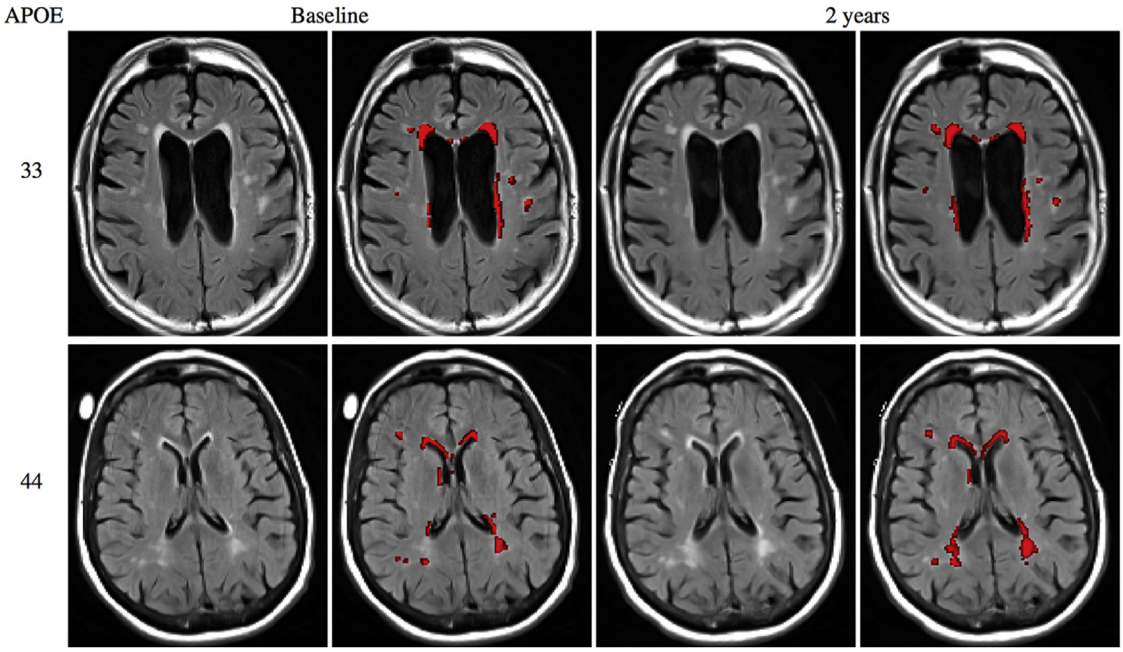

Fig. 3. Longitudinal segmentation for 2 LMCI subjects with *APOE* status 33 (first row) and 44 (second row) with same lesion load at baseline. For each subject, the FLAIR image and the corresponding lesion segmentation (red filled) are presented for the baseline (left) and after 2 years (right). Note the faster rate of accumulation for the homozygous *APOE* ε4 subject (right). Abbreviation: FLAIR, fluid attenuated inversion recovery; LMCI, late mild cognitive impairment. (For interpretation of the references to color in this figure legend, the reader is referred to the Web version of this article.)

ε4ε3 and ε3ε3 groups did not differ significantly from each other. The progression in ε4ε2 group appeared lower than that for the ε4ε3 group, although this was not formally statistically significant ($p = 0.055$). Due to the very small sample size, the CI for the ε4ε2 group was very large. Adjustment for either diagnostic group (model ASTGD) or Aβ status (model ASTGAβ) slightly attenuated the differences between the groups without altering the overall pattern. In the latter model, the dependency of the rate of change on the CSF Aβ level was just formally statistically significant ($p < 0.041$ for interaction with time).

Rates of change also appeared to increase with diagnosis severity (AD > LMCI > EMCI > NC) ($p = 0.03$, model ASTD) ranging from a mean rate of 5.6%/year in the NC to 14.8%/year for the AD. This effect was no longer significant when adjusting additionally for *APOE* status ($p = 0.18$). There was no evidence that diabetes or systolic blood pressure was related to rate of change, and the inclusion of these factors as covariates did not materially alter the pattern of results (see Supplemental Material).

There was no evidence that the length of follow-up influenced the rate of WMH accumulation (p-value >0.5, all tests).

Fig. 3 presents the evolution in WMH for 2 LMCI subjects with the same WMH load at baseline, 1 with ε33 and the other with ε44. Images are shown at baseline and after 2 years.

4. Discussion

This longitudinal study shows a strong association between the *APOE* status and the rate of WMH volume accumulation. We observed an increased rate of change in the homozygous 44 compared to the 33 and 43 carriers in a cohort with relatively low vascular risk factors and WMH burden at baseline. This study included healthy control subjects, people with MCI, and individuals with an AD diagnosis. These findings were observed independently of diagnosis, and when adjusted for CSF Aβ 42 levels, although the latter adjustment did modify the effect size.

In the ADNI study, exclusion criteria were designed to limit the amount of vascular disease using a threshold of 4 on the Hachinski score. Therefore, results obtained from this sample may not necessarily generalize to the population at large. For instance, the change of 22% per year observed for the *APOE* ε4ε4 group might be less likely to occur at higher initial lesion loads (with a larger denominator). The bias toward a vascular risk–free population may further explain why no statistically significant differences at baseline were observed in our sample with respect to *APOE* status. Compared with the general population, this cohort appears enriched in subjects carrying *APOE* ε4 alleles mostly in the MCI group, which may have helped in extracting relevant patterns and allowed the distinction between heterozygous ε4ε3 and homozygous ε4ε4. In addition, the differences observed in terms of study length for the LMCI and AD groups may have led to an underestimation of the observed pattern differences. In the case of the AD population, an additional selection bias might be added since subjects accumulating higher loads of WMH and AD pathology may drop out more quickly than those with few WMH; in ADs, 4 time points may be more difficult to achieve. Despite these potential limitations, a tendency for increased WMH volume and rates of change with diagnostic severity was still observed.

Ensuring the appropriate modeling of biological processes is not trivial. A variety of different ways of modeling change in WMH are used in the literature making comparisons difficult across studies. Most studies calculate absolute changes on an untransformed scale. However, since there is evidence that WMH changes are positively related to baseline WMH volume load in both normal and dementia populations (Sachdev et al., 2007; Schmidt et al., 2003), we chose to analyze changes on a log scale since they implicitly allow the magnitude of absolute change to be related to baseline level.

Our finding that different patterns of WMH evolution were related to *APOE* status is consistent with previously reported results (Godin et al., 2009) in normal aging, with a much higher rate of increase in subjects homozygous for *APOE* ε4 compared with heterozygous subjects or noncarriers. The observation of no

statistically significant difference in rate of change between heterozygous 43 and homozygous 33 may be taken as a possible explanation for disagreements regarding the link of *APOE* ε4 and WMH evolution since in some studies the population was simply dichotomized into carriers and noncarriers (Lo and Jagust, 2012). The different strengths observed with the covariates for the 43 and 33 carriers may reflect potential differences in the pathological process between these 2 groups.

The association between amyloid pathology, *APOE*, and WMH probably reflects the link between Aβ, *APOE* ε4, and CAA (Haglund and Englund, 2002; Verghese et al., 2011). Since a similar tendency was observed after adjustment for diagnostic group or Aβ level, the additional effects of *APOE* on the vasculature, independently of amyloid, are likely to account for the much faster increase in WMH for subjects homozygous ε4 subjects; although amyloid has an independent effect in itself, as indicated by the significant interaction term.

Although the synergetic circle linking WMH, Aβ, and amyloid deposition is widely documented (Donahue and Johanson, 2008; Gupta et al., 2015; Verghese et al., 2011; Zlokovic, 2011), other explanations for the relationships between *APOE* status and WMH have been suggested. The *APOE* ε4 allele has been linked with the permeability of the blood-brain barrier (BBB) and with a decrease in the tight junctions of the blood vessels' endothelium (Nishitsuji et al., 2011). An increased permeability could in turn lead to neuroinflammatory processes, which may contribute to the development of WMH. The dose-dependent association with the number of ε4 alleles could be linked to the hypothesis of the potential protective effect of allele ε3 on the BBB with respect to neuroinflammation (Bell et al., 2012). Furthermore, *APOE* ε4 has been associated with a decrease in glucose uptake, thus leading to deprived regions more vulnerable to ischemia (Alata et al., 2014). *APOE* ε4 homozygotes have also been associated with a reduction in capillary surface (Salloway et al., 2002) in AD; this reduction would directly affect the blood supply in white matter thereby promoting the development of WMH lesions. The association of *APOE* ε4 with microbleeds (Yates et al., 2014) could be related to the exacerbated deleterious effects of vascular risk factors on WM in *APOE* ε4 carriers (De Leeuw et al., 2004; Wang et al., 2015). The possible joint effects and interaction of vascular risk factors such as hypertension and *APOE* ε4 on the blood vessels are therefore in need of further investigation with respect to the development of WMH.

So far, cross-sectional studies have reported contradictory findings regarding the relationship between *APOE* ε4 and WMH. This is further illustrated here by the absence of evidence of a difference across genetic status at baseline while significantly different rates of change were observed. This finding strongly supports the need to better understand the time course and developmental pattern of pathological processes. Cross-sectional studies need to consider age imbalances between groups because it is well understood that increasing age has a strong association with WMH accrual (van Dijk et al., 2008). In our study, we chose to adjust for age as is done in most WMH accrual studies (Godin et al., 2009). This age adjustment explains why the AD group have larger WMH volumes than the somewhat younger late MCI group before (Table 1), but not after age adjustment (Table 2). Limitations of cross-sectional studies may be partially overcome by the application of longitudinal models.

One of the main strengths of this study is the use of a novel longitudinal method of WMH assessment developed for this purpose. The average image on which a generative model is built enables the reduction of measurement noise and accounts for the within-subject correlation. Accounting for such correlation instead of simply applying cross-sectional methods to serial scans for quantitative assessment has been shown to reduce the measurement variability (Reuter et al., 2012). Furthermore, the creation of an average image in a mid-space overcomes the problem of a bias toward a specific time point (Fox et al., 2011; Reuter and Fischl, 2011). Finally, the use of the generative model to constrain the segmentation at each time point allows subtle changes to be measured while maintaining robustness.

This study has a number of limitations. Owing to the complexity of the possible biophysiological interactions between amyloid compounds and apolipoprotein, any statistical conclusions should be treated cautiously. As such, CSF level of Aβ-42 used as a surrogate disease marker for AD pathology (Andreasen et al., 1999) is also known to be related to WMH (Stenset et al., 2006). Use of CSF Aβ-40 measures, more associated to vascular deposition, may be informative of the pathological process. Further work is thus needed to help disentangle WMH progression and CSF Aβ-42 level changes in the pathogenesis of Alzheimer's disease. Moreover, only global WMH loads were considered here, but regional assessment of the lesion growth and differences in pattern across regions could improve our understanding of the complex relationship between *APOE*, AD, and vascular pathology. Allele ε2 carriers were included in this study, and results suggested a protective effect of allele ε2, but the very low prevalence of this allele makes the investigation difficult. Although a similar link between the allele ε2 and WMH has been reported (Gesierich et al., 2016), the very limited number of subjects means our results should be considered very cautiously. In particular, given the 95% CI found for the 42 group (only 6 subjects), the mean negative accrual of WMH cannot be interpreted as significantly different from 0. This is mostly representative of the difficulty to represent relative changes for very small measured volumes. Caution in the interpretation is also warranted here with respect to the ε4 carriers because only 24 homozygous 44 participants were included in the study.

In conclusion, this study shows the impact of *APOE* ε4 on the rate of WMH accrual over and above diagnosis of AD. Carriage of a single ε4 allele with a complementary allele ε3 gave a nonsignificant additional increase of 3% per year, whereas homozygous carriers had a significant additional increase of 16% per year compared with ε3 homozygotes. *APOE* ε4, especially when in the homozygous form, is an important independent factor in the progression of WMH.

Disclosure statement

Frederik Barkhof serves as a scientific consultant to Bayer-Schering, Sanofi-Aventis, Synthon, Novartis, Biogen-IDEC, Merck-Serono, Toshiba Medical systems, Roche, Janssen, TEVA, and Genzyme. He also serves as an editorial board member for Brain, European Radiology, Multiple Sclerosis Journal, Neuroradiology, Radiology, and Neurology. He serves as a consultant for Sanofi-Aventis, Synthon, Janssen, Novartis, Biogen-Idec, Roche, and TEVA; has served on speakers' bureaus for Novartis and Biogen; and receives research support from Neugrid4you (FP7 European committee) and Dutch Foundation for MS Research—centre grant 2010–2014. Nick Fox during the last 2 years has received payment for consultancy or for conducting studies from AVID, IXICO, Janssen Alzheimer Immunotherapy, Sanofi-Aventis, Genentech, Novartis, Roche, and Pfizer/Wyeth Pharmaceuticals. The remaining authors have no conflicts of interest to disclose.

Acknowledgements

C. H. S. is funded by the Wolfson Foundation and the UCL Faculty of Engineering. M. J. C. receives funding from EPSRC (EP/H046410/1). S. O. receives funding from the EPSRC (EP/H046410/1, EP/J020990/1, and EP/K005278), the MRC (MR/J01107X/1), the EU-FP7 project VPH-DARE@IT (FP7-ICT-2011-9-601055), the NIHR Biomedical

Research Unit (Dementia) at UCL, and the National Institute for Health Research University College London Hospitals Biomedical Research Centre (NIHR BRC UCLH/UCL High Impact Initiative-BW.mn.BRC10269). J. B. is an Alzheimer's Research UK Senior Research Fellow. N. F. has an NIHR Senior Investigator award and receives support from the Wolfson Foundation, NIHR Biomedical Research Unit (Dementia) at UCL, the EPSRC, Alzheimer's Research UK, and the NIA. He receives no personal compensation for the activities aforementioned. The Dementia Research Centre is supported by Alzheimer's Research UK, Brain Research Trust, and The Wolfson Foundation. Data collection and sharing for this project was funded by the Alzheimer's Disease Neuroimaging Initiative (ADNI) (National Institutes of Health Grant U01 AG024904) and DOD ADNI (Department of Defense award number W81XWH-12-2-0012). ADNI is funded by the National Institute on Aging, the National Institute of Biomedical Imaging and Bioengineering, and through generous contributions from the following: AbbVie, Alzheimer's Association; Alzheimer's Drug Discovery Foundation; Araclon Biotech; BioClinica, Inc; Biogen; Bristol-Myers Squibb Company; CereSpir, Inc; Eisai Inc; Elan Pharmaceuticals, Inc; Eli Lilly and Company; EuroImmun; F. Hoffmann-La Roche Ltd and its affiliated company Genentech, Inc; Fujirebio; GE Healthcare; IXICO Ltd.; Janssen Alzheimer Immunotherapy Research and Development, LLC; Johnson and Johnson Pharmaceutical Research and Development LLC; Lumosity; Lundbeck; Merck and Co, Inc; Meso Scale Diagnostics, LLC; NeuroRx Research; Neurotrack Technologies; Novartis Pharmaceuticals Corporation; Pfizer Inc; Piramal Imaging; Servier; Takeda Pharmaceutical Company; and Transition Therapeutics. The Canadian Institutes of Health Research is providing funds to support ADNI clinical sites in Canada. Private sector contributions are facilitated by the Foundation for the National Institutes of Health (www.fnih.org). The grantee organization is the Northern California Institute for Research and Education, and the study is coordinated by the Alzheimer's Disease Cooperative Study at the University of California, San Diego. ADNI data are disseminated by the Laboratory for Neuro Imaging at the University of Southern California. The authors would like to thank Alexander Mendelson for his advice on accessing the ADNI data.

Appendix A. Supplementary data

Supplementary data associated with this article can be found, in the online version, at http://dx.doi.org/10.1016/j.neurobiolaging.2017.01.014.

References

Abraham, H.M.A., Wolfson, L., Moscufo, N., Guttmann, C.R.G., Kaplan, R.F., White, W.B., 2016. Cardiovascular risk factors and small vessel disease of the brain: blood pressure, white matter lesions, and functional decline in older persons. J. Cereb. Blood Flow Metab. 36, 132–142.

Alata, W., Ye, Y., St-Amour, I., Vandal, M., Calon, F., 2014. Human apolipoprotein E ε4 expression impairs cerebral vascularization and blood–brain barrier function in mice. J. Cereb. Blood Flow Metab. 35, 86–94.

Andreasen, N., Hesse, C., Davidsson, P., Minthon, L., Wallin, A., Winblad, B., Vanderstichele, H., Vanmechelen, E., Blennow, K., 1999. Cerebrospinal fluid β-amyloid(1-42) in Alzheimer disease. Arch. Neurol. 56, 673.

Bell, R.D., Winkler, E.A., Singh, I., Sagare, A.P., Deane, R., Wu, Z., Holtzman, D.M., Betsholtz, C., Armulik, A., Sallstrom, J., Berk, B.C., Zlokovic, B.V., 2012. Apolipoprotein E controls cerebrovascular integrity via cyclophilin A. Nature 485, 512–516.

Benedictus, M.R., Goos, J.D.C., Binnewijzend, M.A.A., Muller, M., Barkhof, F., Scheltens, P., Prins, N.D., van der Flier, W.M., 2013. Specific risk factors for microbleeds and white matter hyperintensities in Alzheimer's disease. Neurobiol. Aging 34, 2488–2494.

Brickman, A.M., Schupf, N., Manly, J.J., Stern, Y., Luchsinger, J.A., Provenzano, F.A., Narkhede, A., Razlighi, Q., Collins-Praino, L., Artero, S., Akbaraly, T.N., Ritchie, K., Mayeux, R., Portet, F., 2014. APOE ε4 and risk for Alzheimer's disease: do regionally distributed white matter hyperintensities play a role? Alzheimer's Demen. 10, 619–629.

Brundel, M., Kappelle, L.J., Biessels, G.J., 2014. Brain imaging in type 2 diabetes. Eur. Neuropsychopharmacol. 24, 1967–1981.

Cardoso, M.J., Modat, M., Wolz, R., Melbourne, A., Cash, D., Rueckert, D., Ourselin, S., 2015. Geodesic information flows: spatially-variant graphs and their application to segmentation and fusion. IEEE Trans. Med. Imaging 34, 1976–1988.

De Carli, C., Maillard, P., Fletcher, E., 2013. Four Tissue Segmentation in ADNI II. Available at: https://www.alz.washington.edu/WEB/adni_proto.pdf. Accessed February 10, 2017.

De Leeuw, F.E., Richard, F., De Groot, J.C., Van Duijn, C.M., Hofman, A., Van Gijn, J., Breteler, M.M.B., 2004. Interaction between hypertension, apoE, and cerebral white matter lesions. Stroke 35, 1057–1060.

Donahue, J.E., Johanson, C.E., 2008. Apolipoprotein E, amyloid-beta, and blood-brain barrier permeability in Alzheimer disease. J. Neuropathol. Exp. Neurol. 67, 261–270.

Esiri, M., Chance, S., Joachim, C., Warden, D., Smallwood, A., Sloan, C., Christie, S., Wilcock, G., Smith, A.D., 2015. Cerebral amyloid angiopathy, subcortical white matter disease and dementia: literature review and study in OPTIMA. Brain Pathol. 25, 51–62.

Fox, N.C., Ridgway, G.R., Schott, J.M., 2011. Algorithms, atrophy and Alzheimer's disease: cautionary tales for clinical trials. NeuroImage 57, 15–18.

Gesierich, B., Opherk, C., Rosand, J., Gonik, M., Malik, R., Jouvent, E., Hervé, D., Adib-Samii, P., Bevan, S., Pianese, L., Silvestri, S., Dotti, M.T., De Stefano, N., van der Grond, J., Boon, E.M., Pescini, F., Rost, N., Pantoni, L., Lesnik Oberstein, S.A., Federico, A., Ragno, M., Markus, H.S., Tournier-Lasserve, E., Chabriat, H., Dichgans, M., Duering, M., Ewers, M., 2016. APOE ε2 is associated with white matter hyperintensity volume in CADASIL. J. Cereb. Blood Flow Metab. 36, 199–203.

Godin, O., Tzourio, C., Maillard, P., Alpérovitch, A., Mazoyer, B., Dufouil, C., 2009. Apolipoprotein E genotype is related to progression of white matter lesion load. Stroke 40, 3186–3190.

Greenberg, S.M., 2002. Cerebral amyloid angiopathy and vessel dysfunction. Cerebrovasc. Dis. 13 (Suppl 2), 42–47.

Gupta, A., Iadecola, C., York, N., 2015. Impaired Aβ clearance: a potential link between atherosclerosis and Alzheimer's disease. Front. Aging Neurosci. 7, 115.

Haglund, M., Englund, E., 2002. Cerebral amyloid angiopathy, white matter lesions and Alzheimer encephalopathy—a histopathological assessment. Demen. Geriatr. Cogn. Disord. 14, 161–166.

Holland, C.M., Smith, E.E., Csapo, I., Gurol, M.E., Brylka, D.A., Killiany, R.J., Blacker, D., Albert, M.S., Guttmann, C.R.G., Greenberg, S.M., 2008. Spatial distribution of white-matter hyperintensities in Alzheimer disease, cerebral amyloid angiopathy, and healthy aging. Stroke 39, 1127–1133.

Kim, H.J., Ye, B.S., Yoon, C.W., Cho, H., Noh, Y., Kim, G.H., Choi, Y.S., Kim, J.H., Jeon, S., Lee, J.M., Kim, J.S., Choe, Y.S., Lee, K.H., Kim, S.T., Kim, C., Kang, D.R., Ki, C.S., Lee, J.H., Werring, D.J., Weiner, M.W., Na, D.L., Seo, S.W., 2013. Effects of APOE ε4 on brain amyloid, lacunar infarcts, and white matter lesions: a study among patients with subcortical vascular cognitive impairment. Neurobiol. Aging 34, 2482–2487.

Lo, R.Y., Jagust, W.J., 2012. Vascular burden and Alzheimer disease pathologic progression. Neurology 79, 1349–1355.

Modat, M., Cash, D.M., Daga, P., Winston, G.P., Duncan, J.S., Ourselin, S., 2014. Global image registration using a symmetric block-matching approach. J. Med. Imaging 1, 024003.

Modat, M., Ridgway, G.R., Taylor, Z.A., Lehmann, M., Barnes, J., Hawkes, D.J., Fox, N.C., Ourselin, S., 2010. Fast free-form deformation using graphics processing units. Computer Methods Programs Biomed. 98, 278–284.

Mortamais, M., Artero, S., Ritchie, K., 2013. Cerebral white matter hyperintensities in the prediction of cognitive decline and incident dementia. Int. Rev. Psychiatry 25, 686–698.

Nishitsuji, K., Hosono, T., Nakamura, T., Bu, G., Michikawa, M., 2011. Apolipoprotein E regulates the integrity of tight junctions in an isoform-dependent manner in an in vitro blood-brain barrier model. J. Biol. Chem. 286, 17536–17542.

Power, M.C., Deal, J.A., Sharrett, A.R., Jack, C.R., Knopman, D., Mosley, T.H., Gottesman, R.F., 2015. Smoking and white matter hyperintensity progression the ARIC-MRI Study. Neurology 84, 841–848.

Provenzano, F.A., Muraskin, J., Tosto, G., Narkhede, A., Wasserman, B.T., Griffith, E.Y., Guzman, V.A., Meier, I.B., Zimmerman, M.E., Brickman, A.M.; Alzheimer's Disease Neuroimaging Initiative, 2013. White matter hyperintensities and cerebral amyloidosis: necessary and sufficient for clinical expression of Alzheimer disease? JAMA Neurol. 70, 455–461.

Reuter, M., Fischl, B., 2011. Avoiding asymmetry-induced bias in longitudinal image processing. NeuroImage 57, 19–21.

Reuter, M., Schmansky, N.J., Rosas, H.D., Fischl, B., 2012. Within-subject template estimation for unbiased longitudinal image analysis. NeuroImage 61, 1402–1418.

Sachdev, P., Wen, W., Chen, X., Brodaty, H., 2007. Progression of white matter hyperintensities in elderly individuals over 3 years. Neurology 68, 214–222.

Salloway, S., Gur, T., Berzin, T., Zipser, B., Correia, S., Hovanesian, V., Fallon, J., Kuo-Leblanc, V., Glass, D., Hulette, C., Rosenberg, C., Vitek, M., Stopa, E., 2002. Effect of APOE genotype on microvascular basement membrane in Alzheimer's disease. J. Neurol. Sci. 203–204, 183–187.

Schmidt, R., Enzinger, C., Ropele, S., Schmidt, H., Fazekas, F., 2003. Progression of cerebral white matter lesions: 6-year results of the Austrian Stroke Prevention Study. Lancet 361, 2046–2048.

Stenset, V., Johnsen, L., Kocot, D., Negaard, A., Skinningsrud, A., Gulbrandsen, P., Wallin, A., Fladby, T., 2006. Associations between white matter lesions, cerebrovascular risk factors, and low CSF Aβ-42. Neurology 67, 830–833.

Sudre, C., Cardoso, M.J., Bouvy, W., Biessels, G., Barnes, J., Ourselin, S., 2015. Bayesian model selection for pathological neuroimaging data applied to white matter lesion segmentation. IEEE Trans. Med. Imaging 34, 2079–2102.

van Dijk, E.J., Prins, N.D., Vrooman, H.A., Hofman, A., Koudstaal, P.J., Breteler, M.M.B., 2008. Progression of cerebral small vessel disease in relation to risk factors and cognitive consequences: Rotterdam Scan study. Stroke 39, 2712–2719.

Verbeke, G., Molenberghs, G., 2000. Linear Mixed Models for Longitudinal Data. Springer Science & Business Media. Available at: https://books.google.co.uk/books/about/Linear_Mixed_Models_for_Longitudinal_Dat.html?id=nIoME3vzND0C&pgis=1. Accessed January 17, 2016.

Verghese, P.B., Castellano, J.M., Holtzman, D.M., 2011. Apolipoprotein E in Alzheimer's disease and other neurological disorders. Lancet Neurol. 10, 241–252.

Wang, R., Fratiglioni, L., Laukka, E.J., Lövdén, M., Keller, L., Graff, C., 2015. Effects of vascular risk factors and APOE e 4 on white matter integrity and cognitive decline. Neurology 84, 1128–1135.

Wardlaw, J.M., Valdés Hernández, M.C., Muñoz-Maniega, S., 2015. What are white matter hyperintensities made of? Relevance to vascular cognitive impairment. J. Am. Heart Assoc. 4, 1140.

Yates, P.A., Villemagne, V.L., Ellis, K.A., Desmond, P.M., Masters, C.L., Rowe, C.C., 2014. Cerebral microbleeds: a review of clinical, genetic, and neuroimaging associations. Front. Neurol. 4, 205.

Zipfel, G.J., Han, H., Ford, A.L., Lee, J.-M., 2009. Cerebral amyloid angiopathy: progressive disruption of the neurovascular unit. Stroke 40 (3 Suppl), S16–S19.

Zlokovic, B.V., 2011. Neurovascular pathways to neurodegeneration in Alzheimer's disease and other disorders. Nat. Rev. Neurosci. 12, 723–738.